

Robust Fractional Order Proportional, Integral and Derivative Stabilizer for Power Systems

Magdy A.S. Aboelela*, Hisham M. Soliman

Cairo University, Faculty of Engineering, Electric Power and Machines Dept., Giza, Egypt

*Corresponding author, e-mail: aboelelamagdy@yahoo.com

Abstract

This paper focuses on the application of a robust Fractional Order PID (FOPID) stabilizer tuned by Genetic Algorithm (GA). The system's robustness is assured through the application of Kharitonov's theorem to overcome the effect of system parameter's changes within upper and lower limits. The FOPID stabilizer has been approximated during the optimization using the Oustaloup's approximation for fractional calculus and using the "nlpid" toolbox of Matlab during simulation. The objective is to keep robust stabilization with maximum achievable degree of stability against system's uncertainty. This optimization will be achieved with the proper choice of the FOPID stabilizer's parameters (k_p , k_i , k_d , λ , and δ) as discussed later in this article. The optimization has been done using the GA which limits the boundaries of the tuned parameters within the permissible region. The calculations have been applied to a single machine infinite bus (SMIB) power system using Matlab and Simulink. The results show superior behavior of the proposed stabilizer over the traditional PID.

Keywords: power system, power system stabilizer (PSS), genetic algorithm, robust control, single machine infinite bus (SMIB), Kharitonov's theorem, and Matlab/Simulink

Copyright © 2016 Institute of Advanced Engineering and Science. All rights reserved.

1. Introduction

Low or negative damping in a power system can lead to spontaneous appearance of large power oscillations. Several methods for increasing the damping in a power system are available such as static voltage condenser (SVC), high voltage direct current (HVDC) and power system stabilizer (PSS). Operating conditions of a power system are continually changing due to load patterns, electric generation variations, disturbances, transmission topology and line switching [1].

To enhance system damping; the generators are equipped with power system stabilizers that provide supplementary feedback stabilizing signals in the excitation systems [2]. The control strategy should be capable of manipulating the PSS effectively. The PSS should provide robust stability over a wide range of operating conditions, easy to implement, improves transient stability, low developing time and least cost [1]. Various topologies and many control methods have been proposed for PSS design, such as adaptive controller [3], robust controller [4, 5], extended integral controller [6], state feedback controller [7], fuzzy logic controller [8] and variable structure controller [9]. In [10] an adaptive fuzzy PSS that behaves like a PID controller that provides faster stabilization of the frequency error signal with less dependency on expert knowledge is proposed. In [11], an indirect adaptive PSS is designed using two input signals, the speed deviation and the power deviation to a neural network controller.

The robust PSS has the ability to maintain stability and achieves desired performance while being insensitive to the perturbations. Among the various robustness techniques, H_∞ optimal control [12] and the structured singular value (SSV or μ) technique [13] have received considerable attention. But, the application of μ technique for controller design is complicated due to the computational requirements of μ design. Besides the high order of the resulting controller, also introduces difficulties with regard to implementation [14].

The H_∞ optimal controller design is relatively simpler than the μ synthesis in terms of the computational burden [15-16].

Since power systems are highly non-linear, conventional fixed-parameter PSSs cannot cope with wide changes of the operating conditions. There are two main approaches to stabilize a power system over a wide range of operating conditions; namely adaptive control [16-19] and

robust control [20-25]. However, adaptive controllers have generally poor performance during the learning phase; unless they are properly initialized. Successful operation of adaptive controllers requires the measurements to satisfy strict persistent excitation conditions; otherwise the adjustment of the controller's parameters fail [26].

The PSS proposed in this paper belongs to the class of robust controllers. It relies on the Kharitonov theorem and GA optimization. The use of the Kharitonov theorem enables us to consider a finite number of plants to be stabilized. The resulting controller will be able to stabilize the original system at any operating point within the design range. We propose to tune the controller's parameters using the genetic algorithm optimization technique [26].

This article is organized as follows: In section 2, we present a brief introduction to fractional calculus and its approximation. Section 3 presents the GA. Section 4 illustrates the system under investigation. Section 5 presents the problem formulation and the problem solution is discussed in section 6. The design procedure of FOPID PSS is introduced in section 7 with different loading and working conditions. Section 8 and some references are given in section 9. The paper has three appendices A, B, and C.

2. Fractional Order PID Controller ($PI^\lambda D^\delta$) Design

Proportional-Integral-Derivative (PID) controllers are widely being used in industries for process control applications. The merit of using PID controllers lies in its simplicity of design and good performance including low percentage overshoot and small settling time for slow industrial processes. The performance of PID controllers can be further improved by appropriate settings of fractional-I and fractional-D actions.

In a fractional PID controller, the I- and D-actions being fractional have wider scope of design. Naturally, besides setting the proportional, derivative and integral constants K_p , T_d and T_i respectively, we have two more parameters: the power of s in integral and derivative actions- λ and δ respectively. Finding $[k_p, k_i, k_d, \lambda, \text{ and } \delta]$ as an optimal solution to a given process thus calls for optimization on the five-dimensional space. Classical optimization techniques cannot be used here because of the roughness of the objective function surface. We, therefore, use a derivative-free optimization, guided by the collective behavior of social warm and determine optimal settings of $k_p, k_i, k_d, \lambda, \text{ and } \delta$.

The performance of the optimal fractional PID controller is better than its integer counterpart. Thus the proposed design will find extensive applications in real industrial processes. Traces of work on fractional PID controllers are available in the current literature [28-36]. A frequency domain approach based on the expected crossover frequency and phase margin is illustrated in [29]. A method based on pole distribution of the characteristic equation in the complex plane was suggested in [32]. A state-space design method based on feedback poles placement can be viewed in [33].

Moreover, researchers reported that controllers making use of fractional order derivatives and integrals could achieve performance and robustness results superior to those obtained with conventional (integer order) controllers. The Fractional-order PID controller (FOPID) controller is the expansion of the conventional PID controller based on fractional calculus [19, 34].

The differential equation of the $PI^\lambda D^\delta$ controller is described in time domain by

$$u(t) = k_p e(t) + k_i D_t^{-\lambda} e(t) + k_d D_t^\delta e(t) \quad (1)$$

The continuous transfer function of the $PI^\lambda D^\delta$ controller is obtained through Laplace transform as

$$G_c(s) = k_p + k_i s^{-\lambda} + k_d s^\delta \quad (2)$$

It is obvious that the FOPID controller does not only need the design three parameters k_p, k_i and k_d , but also the design of two orders λ, δ of integral and derivative controllers. The orders λ, δ are not necessarily integer, but any real numbers, [27].

3. Genetic Algorithm Operation

To illustrate the working process of genetic algorithm, the steps to realize a basic GA are listed below [35-36]:

Step 1: Represent the problem variable domain as a chromosome of fixed length; choose the size of the chromosome population N , the crossover probability P_c and the mutation probability P_m .

Step 2: Define a fitness function to measure the performance of an individual chromosome in the problem domain. The fitness function establishes the basis for selecting chromosomes that will be mated during reproduction.

Step 3: Randomly generate an initial population of size N : x_1, x_2, \dots, x_N .

Step 4: Calculate the fitness of each individual chromosome: $f(x_1), f(x_2), \dots, f(x_N)$.

Step 5: Select a pair of chromosomes for mating from the current population. Parent chromosomes are selected with a probability related to their fitness. High fit chromosomes have a higher probability of being selected for mating than less fit chromosomes.

Step 6: Create a pair of offspring chromosomes by applying the genetic operators.

Step 7: Place the created offspring chromosomes in the new population.

Step 8: Repeat Step 5 until the size of the new population equals that of initial population, N .

Step 9: Replace the initial (parent) chromosome population with the new (offspring) population.

Step 10: Go to Step 4, and repeat the process until the termination criterion is satisfied.

A GA is an iterative process. Each iteration is called a generation. A typical number of generations for a simple GA can range from 50 to over 500. A common practice is to terminate a GA after a specified number of generations and then examine the best chromosomes in the population. If no satisfactory solution is found, then the GA is restarted [37].

The GA moves from generation to generation until a stopping criterion is met. The stopping criterion could be maximum number of generations, population convergence criteria, lack of improvement in the best solution over a specified number of generations or target value for the objective function.

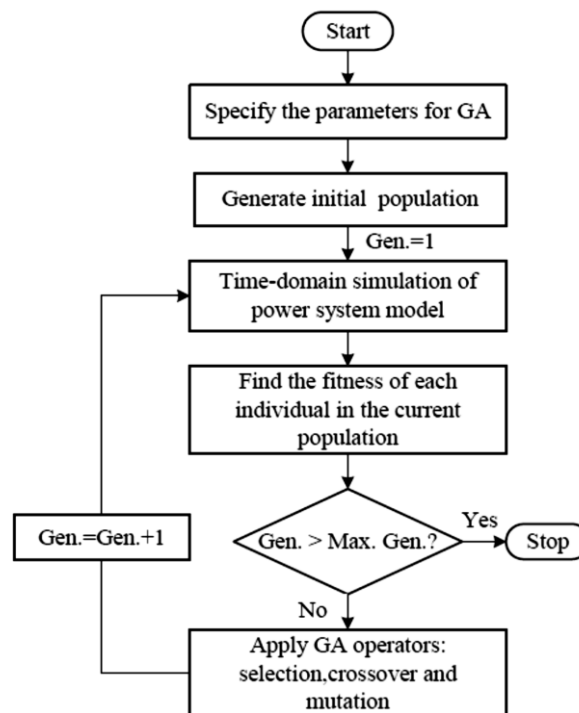


Figure 1. The computational flowchart of the GA

Evaluation functions or objective functions of many forms can be used in a GA so that the function can map the population into a partially ordered set. The computational flowchart of the GA optimization process employed in the present study is given in Figure 1.

4. System Investigated

A single machine-infinite bus (SMIB) system is considered for the present investigations. A machine connected to a large system through a transmission line may be reduced to a SMIB system, by using Thevenin's equivalent of the transmission network external to the machine. Because of the relative size of the system to which the machine is supplying power, the dynamics associated with machine will cause virtually no change in the voltage and frequency of the Thevenin's voltage (infinite bus voltage). The Thevenin equivalent impedance shall hence forth be referred to as equivalent impedance (i.e. $Re+jX_e$) [37-38].

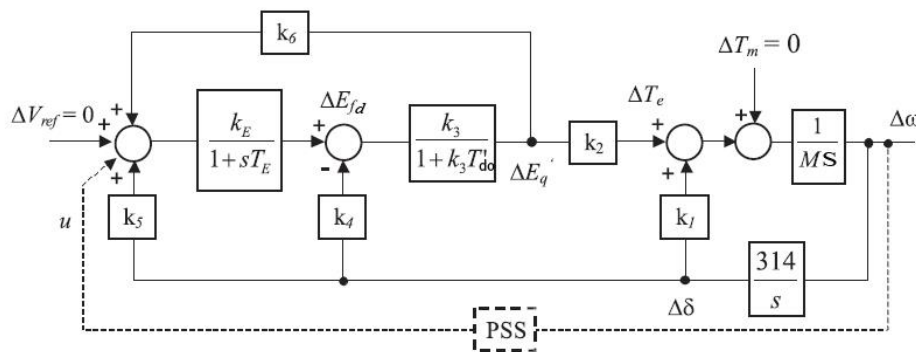


Figure 2. The block diagram for closed loop SMIB System

Figure 2 shows the system under study which consists of a single machine connected to an infinite bus through a tie-line. The machine is equipped with a static exciter. The non-linear equations of the system are

$$\begin{aligned}
 \dot{\omega} &= \frac{T_m - T_e}{M} \\
 \dot{\delta} &= \omega_0 \omega \\
 \dot{E}'_q &= \frac{1}{T_{d0}} \left(E_{fd} - \frac{x_d + x_e}{x_d + x_e} E'_q + \frac{x_d + x'_d}{x_d + x_e} V \cos \delta \right) \\
 \dot{E}_{fd} &= \frac{1}{T_E} (k_E E_{ref} - k_E V_t - E_{fd})
 \end{aligned} \tag{3}$$

The synchronous machine is described as the fourth order model. The two-axis synchronous machine representation with a field circuit in the direct axis but without damper windings is considered for the analysis. The equations describing the steady state operation of a synchronous generator connected to an infinite bus through an external reactance can be linearized about any particular operating point as follows:

$$\Delta T_m - \Delta P = M \frac{d^2 \Delta \delta}{dt^2} \tag{4}$$

$$\Delta P = K_1 \Delta \delta + K_2 \Delta E'_q \tag{5}$$

$$\Delta E'_q = \frac{K_3}{1 + sT'_{d0} K_3} \Delta E_{fd} - \frac{K_3 K_4}{1 + sT'_{d0} K_3} \Delta \delta \tag{6}$$

$$\Delta V_t = K_5 \Delta \delta + K_6 \Delta E'_q \quad (7)$$

The synchronous machine is described by Heffron- Philips model as described in Figure 2. The K-constants are given in appendix A. The data definitions are given in appendix B. The system data are illustrated in appendix C.

The interaction between the speed and voltage control equations of the machine is expressed in terms of six constants k_1 - k_6 . These constants with the exception of k_3 , which is only a function of the ratio of impedance, are dependent upon the actual real and reactive power loading as well as the excitation levels in the machine [37-38].

The system equation can be expressed in the following state variable form [39-40]:

$$\begin{aligned} \dot{X}(t) &= AX(t) + Bu(t) \\ y(t) &= Cx(t) \end{aligned} \quad (8)$$

$$\begin{aligned} X(t) &= [\Delta \delta \quad \Delta \omega \quad \Delta E'_q \quad \Delta E'_{fd}]^T, \\ A &= \begin{bmatrix} 0 & \omega_0 & 0 & 0 \\ \frac{-k_1}{M} & 0 & \frac{k_2}{M} & 0 \\ \frac{k_4}{T'_{do}} & 0 & \frac{1}{T} & -\frac{1}{T'_{do}} \\ \frac{k_5 k_E}{T_E} & 0 & -\frac{k_6 k_E}{T_E} & -\frac{1}{T_E} \end{bmatrix}, \\ B &= \begin{bmatrix} 0 & 0 & 0 & \frac{k_E}{T_E} \end{bmatrix}^T, C = [0 \quad 1 \quad 0 \quad 0]. \end{aligned} \quad (9)$$

5. Problem Formulation

The system can be represented by the block diagram proposed by deMello and Concordia [38] which can be cast as shown in Figure 2. The parameters of the model are load dependent, thus, they have to be calculated at each operating point. Analytical expressions for the parameters k_1 - k_6 , as derived in [15-16], are listed in appendix A. The parameters, k_1 - k_6 , are functions of the loading condition (P and Q). By varying P and/or Q to cover a wide range of system loading, the parameters K_1 to K_6 are computed.

The use of the high-gain voltage regulators usually destabilizes the system. This effect is usually complemented compensated by the inclusion of a stabilizing signal generated by the PSS to provide the required damping. In most cases, the speed deviation signal $\Delta \omega$ is used as an input to the PSS.

To design the PSS, it is convenient to represent the system in the transfer function form as shown in Figure 3. An analytical expression for the transfer function is derived based on the obtained parameters by using Mason's rule. The resulting transfer function is

$$\frac{\Delta \omega}{U}(s) = \frac{bs}{a_4 s^4 + a_3 s^3 + a_2 s^2 + a_1 s + a_0} \quad (10)$$

The transfer-function coefficients expressed in terms of the k -parameters are:

$$\begin{aligned} a_4 &= M T T_E \\ a_3 &= M(T + T_E) \\ a_2 &= M = 314 k_1 T T_E + k_E k_3 k_6 M \\ a_1 &= 314 k_1 (T + T_E) - 314 k_2 k_3 k_4 T_E \\ a_0 &= 314 (k_1 - k_2 k_3 k_4 + k_E k_1 k_3 k_6) \\ b &= k_E k_2 k_3 \end{aligned} \quad (11)$$

The coefficients of the transfer function are load-dependent. So, the PSS has to be adjusted at different loads. To scan the whole range of operation, the load dependency may require the analysis of a large number of points with a new model generated at each operating condition.

A proposed technique, based on the Kharitonov theorem and GA, is used to design a fixed parameters robust FOPID controller to stabilize the non-linear system over the specified range of operating conditions $[P_{\min}, P_{\max}]$ and $[Q_{\min}, Q_{\max}]$. In this technique, the problem is transformed to simultaneous stabilization of a finite number of extreme plants. We will show in the next section that we need to stabilize exactly eight characteristic polynomials.

5.1. Mathematical Tools and Problem Solution

5.1.1. Kharitonov Theorem

The Kharitonov theorem studies the robust stability of an interval polynomial family [40]. A polynomial is said to be an interval polynomial if each coefficient a_i is independent of the others and varies within an interval having lower and upper bounds that is,

$$p = a_n s^n + a_{n-1} s^{n-1} + \dots + a_0 \quad (12)$$

$$a_i = [a_i^-, a_i^+] \quad (13)$$

The Kharitonov theorem states that "An interval polynomial is robustly stable if and only if the following four Kharitonov polynomials are stable.

$$p = \sum_{i=0}^n [a_i^-, a_i^+] s^i \quad (14)$$

$$\begin{aligned} p_1 &= a_0^- + a_1^- s + a_2^+ s^2 + a_3^+ s^3 + a_4^- s^4 + \dots \\ p_2 &= a_0^+ + a_1^+ s + a_2^- s^2 + a_3^- s^3 + a_4^+ s^4 + \dots \\ p_3 &= a_0^+ + a_1^- s + a_2^- s^2 + a_3^+ s^3 + a_4^+ s^4 + \dots \\ p_4 &= a_0^- + a_1^+ s + a_2^+ s^2 + a_3^- s^3 + a_4^- s^4 + \dots \end{aligned} \quad (15)$$

Assuming that the coefficient function a_i depends continuously on the vector $= [P \ Q]^T$ (machine loading P and Q), we define the bounds and simply construct the polynomial described by

$$\begin{aligned} a_i^{*-} &= \min_r(a_i) \\ a_i^{*+} &= \max_r(a_i) \end{aligned} \quad (16)$$

$$p^*(s) = \sum_{i=0}^n [a_i^{*-}, a_i^{*+}] s^i \quad (17)$$

Then the robust stability of polynomial (30) implies the robust stability of (12).

5.1.2. Oustaloup's Recursive Filter to Approximate FOPID

Some continuous filters have been summarized in [41]. Among the filters, the well-established Oustaloup recursive filter has a very good fitting to the fractional-order differentiators. Assume that the expected fitting range is (ω_b, ω_h) . The filter can be written as

$$G_f(s) = K \prod_{k=-N}^N \frac{s + \omega_k'}{s + \omega_k} \quad (18)$$

where the poles, zeros, and gain of the filter can be evaluated such that

$$\begin{aligned} \omega_k' &= \omega_b \left(\frac{\omega_h}{\omega_b} \right)^{\frac{k+N+\frac{1}{2}(1-\gamma)}{2N+1}} \\ \omega_k &= \omega_b \left(\frac{\omega_h}{\omega_b} \right)^{\frac{k+N+\frac{1}{2}(1+\gamma)}{2N+1}} \end{aligned} \quad (19)$$

and

$$K = \omega_h^\gamma$$

Thus, the any signal $y(t)$ signal can be filtered through this filter and the output of the filter can be regarded as an approximation for the derivative term of the FOPID with $\gamma=\delta$ or the integral counterpart with $\gamma=-\lambda$. The resulted transfer function of the FOPID is the sum of the proportional term k_p plus the filter approximation of the integral term ($k_i s^{-\lambda}$) plus the derivative term ($k_D s^\delta$). The result will be the approximated transfer function of the FOPID controller $G_c(s)$ as given by equation (2).

In general $G_c(s)$ can be assumed to be in the form:

$$G_c(s) = \frac{N(s)}{D(s)} \quad (20)$$

As shown in Figure 3, the closed loop characteristic equation can be written as

$$1 + G_c(s)G_p(s) = 0 \quad (21)$$

Where $G_p(s) = \frac{\Delta\omega}{U}(s)$ is the plant transfer function [18].

5.1.3. The 16 Kharitonov Polynomials

Given the plant family with Kharitonov polynomials N_1, \dots, N_4 and D_1, \dots, D_4 for the numerator and denominator, respectively, we define the 16 Kharitonov plants as [42]

$$G_c^i(s) = \frac{N_{i_1}(s)}{D_{i_2}(s)}, i_1 = 1, 2, \dots, 4 \text{ and } i_2 = 1, 2, \dots, 4 \quad (22)$$

Where $i=1, 2, \dots, 16$. If the controller can stabilize all the 16 closed loop polynomials given as

$$1 + G_c^i(s)G_p(s) = 0 \quad (23)$$

Then the closed loop system (33) is robustly stable, where $i_1 = 1, 2, \dots, 4$ and $i_2 = 1, 2, \dots, 4$.

Applying the above mathematical tools to the single machine–infinite bus system (Figure 1), we have the vector r which is composed of two independent components.

$$r = [P \quad Q]^T \quad (24)$$

In the system under study, the numerator of the transfer function is a first order polynomial (bs). Thus, the coefficient b has two extreme values b^+ and b^- ; that is, the 16 plants corresponding to (23) are reduced to 8 plants only.

6. Problem Solution

To stabilize the system over the required ranges of P and Q , the following eight polynomials must be stable.

We will use the genetic algorithm to find the values of k_p , k_i , k_d , λ , and δ that correspond to the following optimization problem

$$\min_{k_p, k_i, k_d, \lambda, \text{ and } \delta} (\max(\lambda_e)) \quad (25)$$

Subject to

$$\begin{aligned} k_p^{\min} &\leq k_p \leq k_p^{\max} \\ k_i^{\min} &\leq k_i \leq k_i^{\max} \\ k_D^{\min} &\leq k_D \leq k_D^{\max} \\ \lambda^{\min} &\leq \lambda \leq \lambda^{\max} \\ \gamma^{\min} &\leq \gamma \leq \gamma^{\max} \end{aligned} \quad (26)$$

where λ_e is a vector containing the real parts of the roots of the eight equations resulting from (25). This means that the parameters k , z and p must stabilize the eight polynomials in Equation (25). On the other hand, the swarm optimization algorithm attempts to push the closed-loop poles to the left as far as possible by minimizing the maximum real part of the roots resulting from (25). The problem can be tackled using a different approach.

If we divide the range of P and Q into small steps, the resulting grid will represent the possible operating points.

For each point on the grid, a model can be derived. Applying the genetic algorithm optimization technique to stabilize such systems is possible. However, there is no guarantee that stability is preserved for intermediate points inside the grid. The proposed technique eliminates this short coming via the Kharitonov theorem.

7. PSS Design for Different Machine Loadability

The design objective, in this paper, is to implement the machine load ability, of the system under study, over the range $Q \in [-0.4, 0.4]$ and $P \in [0.2, 1.2]$. The design procedure can be summarized as follows:

- Develop the linearized model as shown in Figure 2. The machine parameters and the k -parameter calculations are given in the Appendices A and C.
- Based on the analytical expressions for a_0, a_1, \dots, a_4 and b in (11), calculate the maximum and minimum values of the aforementioned parameters using any standard optimization technique. Note that a_3 and a_4 do not depend on the values of P and Q .
- Using (29) and replacing a_i by a_i^* , construct the four Kharitonov's polynomials as in (15). Compute the roots of the 8 extreme polynomials and take the largest real part of the roots as the objective function to be minimized.
- Use the GA to find a solution for the optimization problem (26) such that the roots of (25) lie in the left hand side of the s -plane away from the imaginary axis as much as possible. Thus the shortest settling time of oscillations is achieved

The above procedure is applied to the system under study as follows: Consider the system transfer function (10). The extreme values of its coefficients are calculated as

$$\begin{aligned} a_i^{*-} &= \min_{P,Q}(a_i) \text{ and } a_i^{*+} = \max_{P,Q}(a_i) \\ b_i^{*-} &= \min_{P,Q}(b_i) \text{ and } b_i^{*+} = \max_{P,Q}(b_i) \end{aligned} \quad (27)$$

The results of the above calculations are

$$\begin{aligned} a_4^* &= 1, a_3^* = 22, a_2^* \in [64 \ 106], a_1^* \in [388 \ 1002], \\ a_0^* &[392 \ 2624] \text{ and } b^* \in [2.7 \ 12.4] \end{aligned}$$

Then, the four Kharitonov polynomials are:

$$\begin{aligned} p_1 &= 392 + 388s + 106s^2 + 22s^3 + s^4 \\ p_2 &= 2624 + 1003s + 64s^2 + 22s^3 + s^4 \\ p_3 &= 2624 + 388s + 64s^2 + 22s^3 + s^4 \\ p_4 &= 392 + 1003s + 106s^2 + 22s^3 + s^4 \end{aligned} \quad (28)$$

7.1. Design of a Robust PSS using GA

The plant transfer function (10) is analyzed using eight extreme plants given by

$$\begin{aligned} G_p(s) &= \frac{\Delta\omega}{U}(s) = \frac{b^-s}{p_i}, i = 1, 2, \dots, 4 \\ G_p(s) &= \frac{\Delta\omega}{U}(s) = \frac{b^+s}{p_i}, i = 1, 2, \dots, 4 \end{aligned} \quad (29)$$

To reach the optimization goal, proper adjustment of the GA parameters are needed. This requires the determination of population size ($N=100$ is sufficient), the bit size for each binary parameter (16 is reasonable size), and the upper and lower bounds of the optimization of

FOPID PSS (for k_p , k_i , and k_d), [0 100] is an acceptable range but for λ and δ [0 1.5] is found to be a proper choice in our case [43].

The results obtained using the GA on FOPID PSS design procedure mentioned in this paper are delineated in Table 1. The same procedure can be successfully applied to the case of PID PSS considering the limits of λ and δ of the FOPID PSS as [1 1]. Results of this case are also shown in Table 1.

The proposed PSS is tested over three operating condition.

7.2. The Normal Loading Test

The first operating point is $P = 0.8$ pu and $Q = 0.3$ pu represents the normal loading conditions. The system was exposed to a 0.20 p.u step increase in the input torque reference at 0.5 s. The disturbance was removed at 15 s, .e. the signal duration is 14.5 s, and the system returned to the original operating point by the end of disturbance. The regulated system without a stabilizer is stable at this point [18]. However, the mechanical disturbance pushes the system close to the stability bound. Figure 3 shows the machine speed deviation and the machine power angle (δ). It is clear that if the power system stabilizer is not employed, the rotor angle oscillation will have a very slow damping behavior. On the other hand, the proposed FOPID stabilizer successfully suppresses and damps the oscillations in almost three seconds. The controller signal is shown in Figure 3. It is clear that the controller is utilizing the full control range limited by the maximum standard power system stabilizer signal ± 0.1 pu.

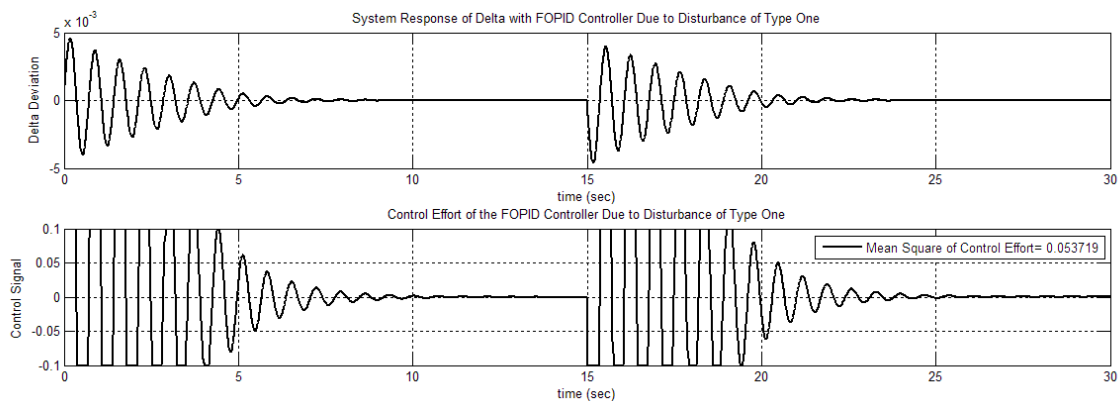


Figure 3. System response to 0.2 pu torque disturbance at ($P = 0.8$, $Q = 0.3$)

The Simulink models for the FOPID PSS applications are illustrated in Figures (4) and (5). The FOPID PSS block is represented by “NIPID” block of “ninteger” blockset of Matlab [44].

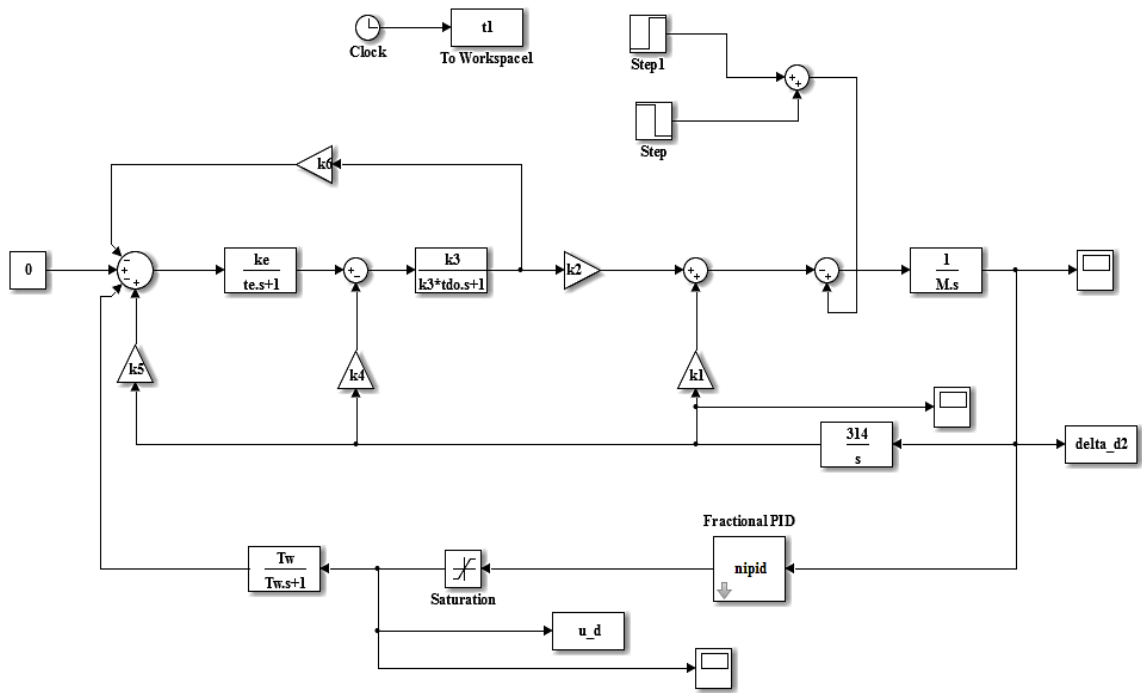


Figure 4. Matlab/Simulink Model with FOPID PSS and Torque Disturbance Signal

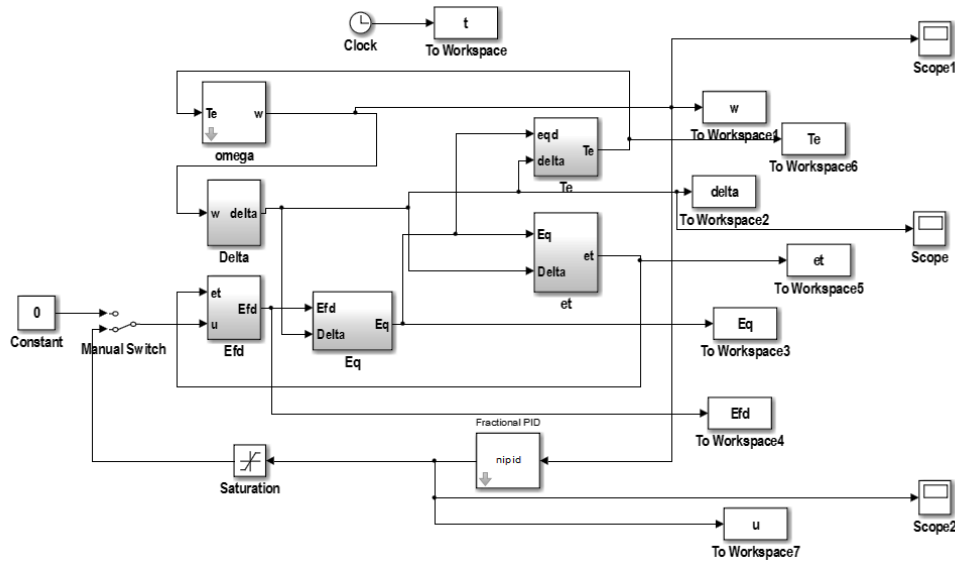


Figure 5. Matlab/Simulink Model of SMIB with FOPID PSS

Table 1. GA estimated parameters for PID and FOPID PSS

Controller	k_p	k_i	k_d	δ	λ
PID (minimum=-1.3961)	45.36	45.452	62.2	N/A	N/A
FOPID (minimum= -1.3849)	48.50	93.666	79.8	0.61	1.3

7.3. Overload Test

In this test the machine was operating at $P = 1.2$ pu and $Q = 0.2$ pu. The machine speed deviation is unstable at this operating point [18]. Figure 6 shows the effectiveness of the proposed FOPID PSS to stabilize the system during over loading conditions [45].

7.4. Full Load with Leading Power Factor Test

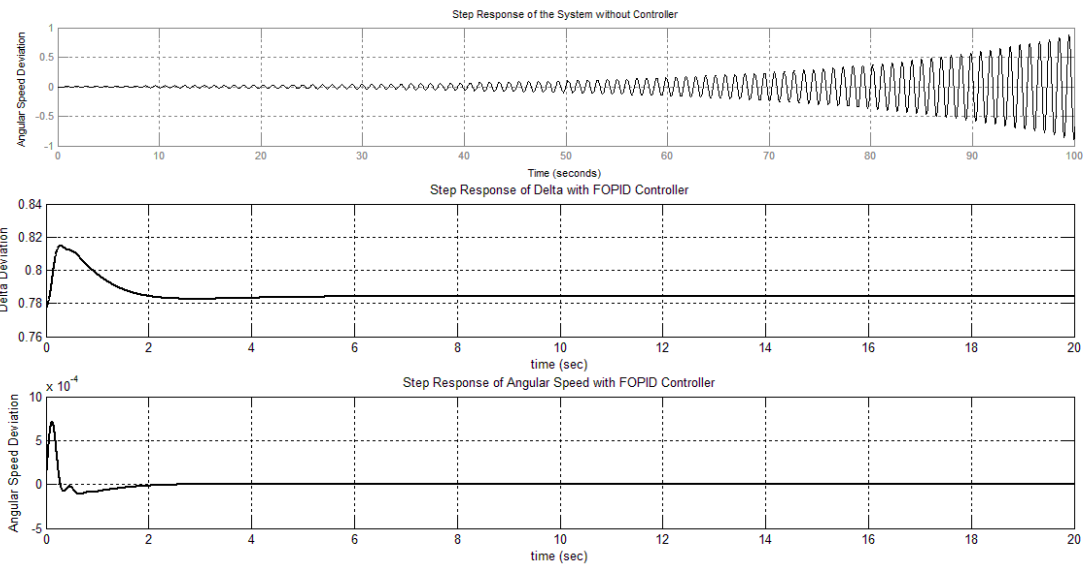


Figure 6. $\Delta\delta$ and $\Delta\omega$ after adding FOPID PSS type in normal operation at ($P = 1.2, Q = 0.2$)

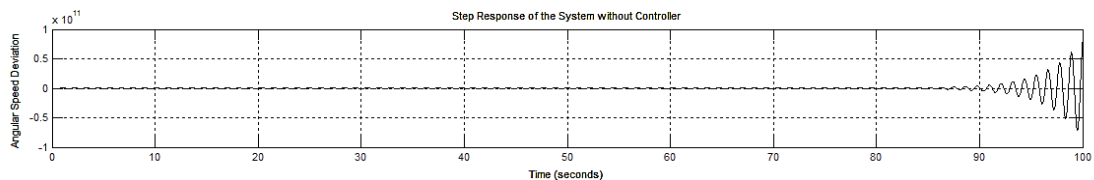


Figure 7a. $\Delta\delta$ without Controller ($P = 1, Q = -0.4$)

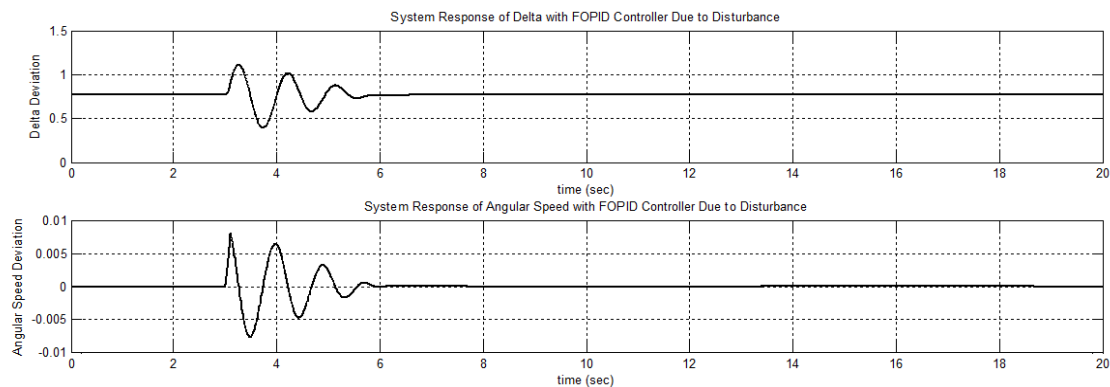


Figure 7b. $\Delta\delta$ and $\Delta\omega$ due to a three line to ground fault at 3 s staying for 100 ms after adding FOPID PSS type ($P = 1, Q = -0.4$)

The second operating point is $P = 1$ pu and $Q = -0.4$ pu. This point lies in the unstable region for the regulated system without a stabilizer as illustrated in Figure 7a. The system at this operating point was exposed to a three phase to ground short circuit at 3 seconds and this will stay only for 100 m-seconds and then cured. Figure 7b illustrates that the proposed FOPID stabilizer can damp the power angle and angular frequency oscillations within a short period of time with the same value of tuned parameters given in Table 1.

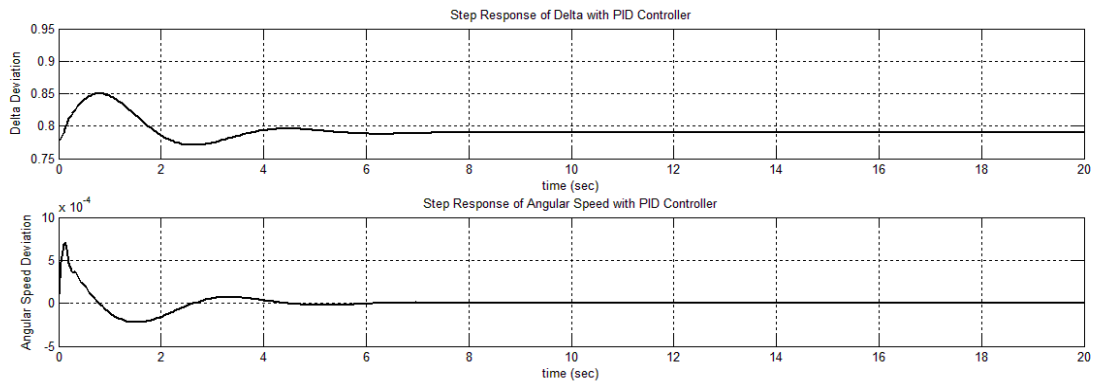


Figure 8. $\Delta\delta$ and $\Delta\omega$ after adding PID PSS type in normal operation ($P = 0.8$, $Q = 0.3$)

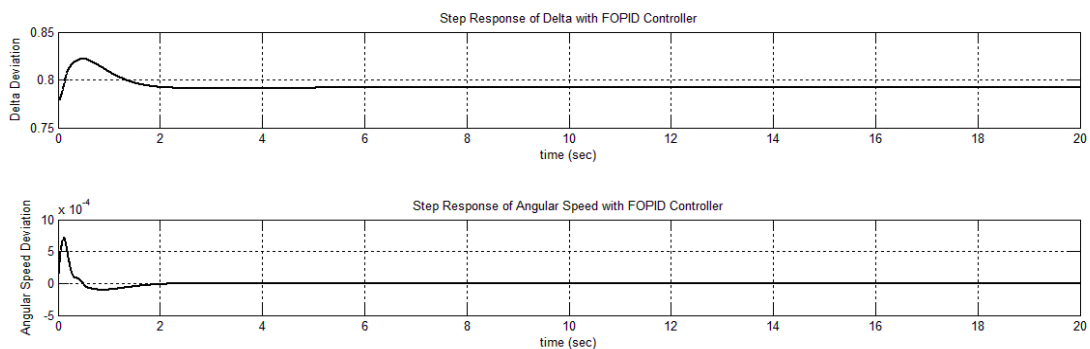


Figure 9. $\Delta\delta$ and $\Delta\omega$ after adding FOPID PSS type in normal operation ($P = 0.8$, $Q = 0.3$)

Finally, for the more illustration, the effect of the PID and FOPID PSSs on the stabilization of the SMIB power system described here in is shown in Figures (8) and (9) for only the case of normal operation with $P = 0.8$ pu and $Q = 0.3$ pu without disturbance. It is clear that the damping effect of the FOPID PSS is noticeable compared with that of the PID PSS. The control effort in both PID and FOPID PSSs are shown in Figures 10a and 10b. Obviously, the control effort of the FOPID PSS is much less than that of the PID in both magnitude and mean square error.

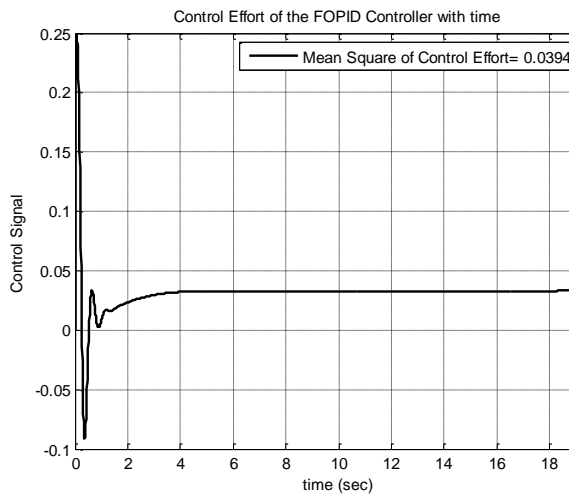


Figure 10a. Control Effort of the FOPID PSS in normal operation ($P = 0.8, Q = 0.3$)

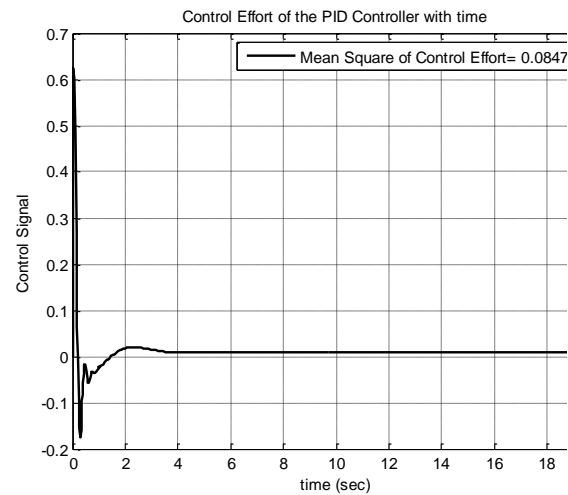


Figure 10b. Control Effort of the PID PSS in normal operation ($P = 0.8, Q = 0.3$)

Moreover, the minimum negative eigen value of the stabilized SMIB system using the PID and FOPID PSS is almost the same as shown in Table 1. The change of this value for the case of FOPID PSS with iteration is delineated in Figure 11.

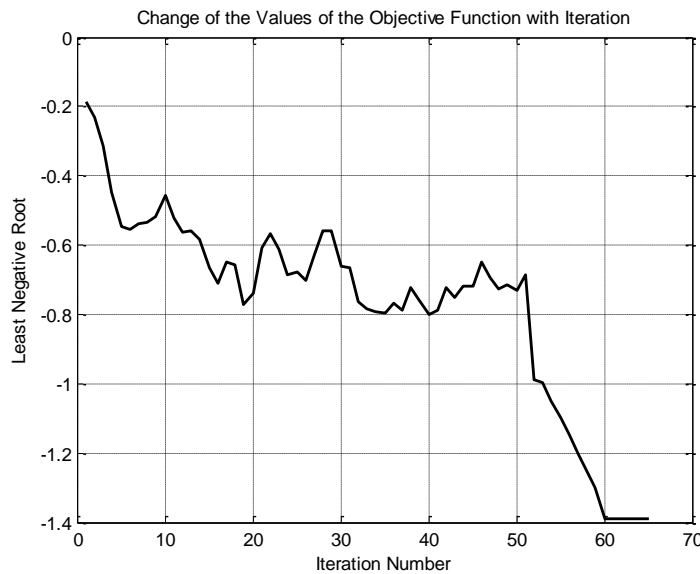


Figure 11. The Objective Function vs. Iterations in case of FOPID PSS

8. Conclusion

The design of a robust FOPID PSS using the Kharitonov theorem has been proposed. The k -parameters of the model are parameterized in terms of the operating point (P, Q). Accordingly, the coefficients 'bounds of the transfer function relating the stabilizing control signal to the speed deviation have been calculated over the whole range of operating points. The design is based on simultaneous stabilization of eight extreme plants to achieve a satisfactory dynamic performance. The calculations are based on the GA optimization algorithm. Simulation results based on a non-linear model of the power system confirm the ability of the proposed compensator to stabilize the system over a wide range of operating points as illustrated with various examples.

The performance of the conventional PID PSS, designed with the same procedure, as compared with the FOPID PSS shows less oscillation damping of both the changes in angle δ and the angular speed ω .

References

- [1] Lee SS, Park JK. *Design of reduced order observer based variable structure power system stabilizer for immeasurable state variables*. IEE Proc. Conf. Transm. Distrib. 1998; 145(5): 525-530.
- [2] Mrad F, Karaki S, Copti B. *An adaptive fuzzy synchronous machine stabilizer*. IEEE Trans. Syst. Man. Cybern, 2000; 30(1): 131-137.
- [3] Shamsollahi P, Malik OP. Adaptive control applied to synchronous generator. IEEE Trans. On Ene. Conv. 1999; 14(4): 1341-1346.
- [4] Doyle JC, Francis BA, Tannenbaum AR. *Feedback control theory*. Macmillan Press, New York, 1992
- [5] Duc. G, Font. S. *H[∞] theory μ -analyse, tools for robustness*. HERMES Science Publications. Paris. 1999. p. 47- 60 (in French).
- [6] Mat lab Help Documentation Release 12, *Math works*, USA.
- [7] MacFarlane DC, Glover K. A loop shaping design procedure using H[∞] synthesis. *IEEE Trans. Auto. Control*, 1992, Vol. AC-37: 759–769.
- [8] Chen G, Malik OP. Tracking constrained adaptive power system stabilizer. *IEE Proceedings, Generation, Transmission and Distribution*, 1995; 142: 149–156.
- [9] Gosh A, Ledwich MO, Hope G. Power system stabilizers based on adaptive control techniques. *IEEE Transactions on Power Apparatus and Systems, PAS-103*. 1989; 8: 983–989.
- [10] Kothari ML, Bhattacharya K, Nada J. Adaptive power system stabilizer based on pole shifting technique. *IEE Proceedings*, 1996; 143(1): 96–98.
- [11] Malik OP, Chen G, Hope G, Qin Y, Xu G. *An adaptive self-optimizing pole shifting control algorithm*. IEE Proceedings of D, 1992; 139: 429–438.
- [12] Chen S, Malik OP. *H optimization-based power system stabilizer design*. IEE Proceedings, Generation, Transmission and Distribution. 1995; 142: 179–184.
- [13] Samarasinghe VG, Pahalawaththa NC. *Damping of multimodal oscillations in power systems using variable structure control techniques*. IEE Proceedings of Generation, Transmission and Distribution. 1997; 144(3): 323–331.
- [14] Shu H, Chen T. *Robust digital design of power system stabilizers*. Proceedings of the American Control Conference, Albuquerque, 1997: 1953–1957.
- [15] Soliman H, Elshafei AL, Shaltout AA, Morsi MF. *Robust power system stabilizer*. IEE Proceedings, Generation, Transmission and Distribution. 2000; 147(5): 285–291.
- [16] Soliman HM, Sakr, MMF. *Wide-range power system pole placer*. IEE Proceedings. 1988; 135(3): 95–101.
- [17] Sun C, Zhao Z, Sun Y, Lu Q. *Design of non-linear robust excitation control for multi-machine power system*. IEE Proceedings, Generation, Transmission and Distribution. 1996; 143: 253–257.
- [18] El-Metwally KA, Elshafei AL, Soliman HM. A robust power-system stabilizer design using swarm optimization. *Int. J. Modeling, Identification and control*. 2006; 1(4).
- [19] Aboeela MAS, Ahmed MF, Dorrah HT. Design of aerospace control systems using fractional PID controller. *Journal of Advanced Research*. 2012; 3(2): 185-192.
- [20] Petras I, Podlubny I, O'Leary P, Dorcak L, Vinagre BM. Analogue realizations of fractional-order controllers. *Nonlinear Dynamics*. 2002; 29: 281- 296.
- [21] Vinagre BM, Podlubny I, Dorcak L, Feliu V. *On fractional PID controllers: A frequency domain approach*. Proc. Of IFAC Workshop on Digital Control – Past, Present and Future of PID Control, 2000: 53-58.
- [22] Milos S, Martin C. *The fractional order PID controller outperforms the classical one*. 7th International Scientific-Technical Conference – PROCESS CONTROL2006; June 13-16, 2006, Koutynad Desnou, Czech Republic.
- [23] Podlubny I, Petras I, Vinagre BM, Chen Y, O' Leary P, Dorcak L. Realization of fractional order controllers. *Acta Montanistica Slovaca*. 2003; 8.
- [24] Petras I. The fractional order controllers: Methods for their synthesis and application. *Journal of Electrical Engineering*. 50(9): 284-288.
- [25] Dorcak L, Petras I, Kostial I, Terpak J. *Statespace controller design for the fractional-order regulated system*. Proc. Of the International Carpathian Control Conference. 2001: 15-20.
- [26] Podlubny I. Fractional-order systems and PI ^{λ} D ^{δ} controllers. *IEEE Trans. On Automatic Control*. 1999; 44(1): 208-213.
- [27] Petras I, Dorcak L, Kostial I. *Control quality enhancement by fractional order controllers*. 2nd National Conference on Recent Trends in Information Systems (ReTIS-08) controllers, Acta Montanistica Slovaca, 1998; 3(2): 143-148.
- [28] Podlubny I, Petras I, Vinagre BM, O' Leary P, Dorcak L. Analogue realizations of fractional-order controllers. *Nonlinear Dynamics*. 2002; 29: 281-296.

- [29] Vinagre BM, Podlubny I, Dorcak L, Feliu V. *On fractional PID controllers: A frequency domain approach*. Proc. Of IFAC Workshop on Digital Control – Past, Present and Future of PID Control. 2000: 53-58.
- [30] Milos S, Martin C. *The fractional order PID controller outperforms the classical one*. 7th International Scientific-Technical Conference –PROCESS CONTROL 2006, June 13-16, 2006, Koutynad Desnou, Czech Republic.
- [31] Podlubny I, Petras I, Blas Vinagre BM, Chen Y, O'Leary P, Dorcak L. Realization of fractional order controllers. *Acta Montanistica Slovaca*. 2003; 8.
- [32] Petras I. The fractional order controllers: Methods for their synthesis and application. *Journal of Electrical Engineering*. 1999; 50(9-10): 284-288.
- [33] Dorcak L, Petras I, Kostiall, Terpak J. *Statespace controller design for the fractional-order regulated system*. Proc. Of the International Carpathian Control Conference. 2001: 15-20.
- [34] Petras I, Vinagre BM. Practical application of digital fractional-order controller to temperature control. *Acta Montanistica Slovaca*. 2002; 7(2): 131-137.
- [35] Goldberg DE. *Genetic Algorithms in Search optimization and Machine Learning*. Reading, MA: Addison-Wesley Publishing Company, Inc. 1991
- [36] Koza JR. Genetic evolution and co-evolution of computer programs. In Langton, CGC Taylor, JD Farmer and S Rasmussen (Eds. *Artificial Life II: SFI Studies in the Sciences of Complexity*. 10. Addison-Wesley, 1991.
- [37] Rashidi M, Rashidi F, Monavar H. *Tuning of power system stabilizers via genetic algorithm for stabilization of power systems*. Proceedings of the IEEE International Conference on Systems, Man & Cybernetics: Washington, D.C., USA. 2003: 649-654.
- [38] deMello FP, Concordia C. Concepts of synchronous machine stability as affected by excitation control. *IEEE Transactions on Power Apparatus and Systems, PAS-88*. 1969: 316–327.
- [39] Barmish BR. *New Tools for Robustness of Linear Systems*. Macmillan Publisher. 1994.
- [40] Xue D, Chen Y, Atherton DP. *Linear Feedback Control. Society for Industrial and Applied Mathematics*, Philadelphia. 2007.
- [41] Barmish BR. *New Tools for Robustness of Linear Systems*. Macmillan Publisher. 1994.
- [42] Goldberg DE. *Algorithms in Search, Optimization, and Machine Learning. Addison-Wiley Publishing Company, Inc.* 1989.
- [43] Valerio D, De Costa JS. *Ninteger: a fractional control toolbox for Mat lab*. In First IFAC workshop on fractional differentiation and its applications. Bordeaux: IFAC, 2004b.
- [44] Klein, M, Rogers GJ, Moorty S, Kundur P. Analytical investigation of factors influencing PSS Performance. *IEEE Transaction on EC*. 1992; 7(3): 382–390.
- [45] Kundur P. *Power System Stability and Control*. McGraw-Hill, 1994.

Appendix A Derivation of k-constants

All the variables with subscript 0 are values of variables evaluated at their pre-disturbance steady-state operating point from the known values of P_0 , Q_0 and V_{t0} .

$$i_{q0} = \frac{P_0 V_{t0}}{\sqrt{(P_0 x_q)^2 + (V_{t0}^2 + Q_0 x_q)^2}} \quad (A1)$$

$$v_{d0} = i_{q0} x_q \quad (A2)$$

$$v_{q0} = \sqrt{V_{t0}^2 - v_{d0}^2} \quad (A3)$$

$$i_{d0} = \frac{Q_0 + x_q i_{q0}^2}{v_{q0}} \quad (A4)$$

$$E_{q0} = v_{q0} + i_{d0} x_q \quad (A5)$$

$$E_0 = \sqrt{(v_{d0} + x_e i_{q0})^2 + (v_{q0} - x_e i_{d0})^2} \quad (A6)$$

$$\delta_0 = \tan^{-1} \frac{(v_{d0} + x_e i_{q0})}{(v_{q0} - x_e i_{d0})} \quad (A7)$$

$$K_1 = \frac{x_q - x_d}{x_e + x_d} i_{q0} E_0 \sin \delta_0 + \frac{E_{q0} E_0 \cos \delta_0}{x_e + x_q} \quad (A8)$$

$$K_2 = \frac{E_0 \sin \delta_0}{x_e + x_d} \quad (A9)$$

$$K_3 = \frac{x_d + x_e}{x_d + x_e} \quad (A10)$$

$$K_4 = \frac{x_q - x_d}{x_e + x_d} E_0 \sin \delta_0 \quad (A11)$$

$$K_5 = \frac{x_q}{x_e + x_q} \frac{v_{d0}}{V_{t0}} E_0 \cos \delta_0 - \frac{x_d}{x_e + x_d} \frac{v_{q0}}{V_{t0}} E_0 \sin \delta_0 \quad (A12)$$

$$K_6 = \frac{x_e}{x_e + x_d} \frac{v_{q0}}{V_{t0}} \quad (A13)$$

Appendix B

Nomenclature

All quantities are per unit on machine base.

D	Damping Torque Coefficient
M	Inertia constant
ω	Angular speed
δ	Rotor angle
i_d, i_q	Direct and quadrature components of armature current
x_d and x_q	Synchronous reactance in d and q axis
x_d' and x_q'	Direct axis and Quadrature axis transient reactance
E_{fd}	Equivalent excitation voltage
K_E	Exciter gain
	Exciter time constant

T_E	Mechanical and Electrical torque
T_m and T_e	Field open circuit time constant.
T_{d0}	Direct and quadrature components of terminal voltage
V_d and V_q	Change in T_e for a change in δ with constant flux linkages in the d axis
K1	Change in T_e for a change in d axis flux linkages with constant δ
K2	Impedance factor
K3	Demagnetizing effect of a change in rotor angle
K4	Change in V_t with change in rotor angle for constant E_q'
K5	Change in V_t with change in E_q' constant rotor angle
K6	

Appendix C

The system data are as follows:

Machine (p.u):

$$\begin{aligned}
 x_d &= 1.6 & x_d' &= 0.32 \\
 x_q &= 1.55 & T_{d0}' &= 6 \text{ s} \\
 D &= 0.0 & M &= 10 \text{ s}
 \end{aligned} \tag{C1}$$

Transmission line (p.u):

$$r_e = 0.0 \quad x_e = 0.4 \tag{C2}$$

Exciter:

$$K_E = 25.00 \quad T_E = 0.05 \text{ s} \tag{C3}$$

Nominal Operating point:

$$\begin{aligned}
 V_{t0} &= 1.0 & P_0 &= 0.8 \\
 Q_0 &= 0.3 & \delta_0 &= 45^\circ \\
 \omega_0 &= 314
 \end{aligned} \tag{C4}$$

Others (C5)

$$\begin{aligned}
 k_3 &= 1/2.78 \\
 v &= 1.0 \\
 T_w &= 5
 \end{aligned}$$